Cement and Concrete Research 38 (2008) 1409–1415

Contents lists available at ScienceDirect

Cement and Concrete Research

journal homepage: http://ees.elsevier.com/CEMCON/default.asp

Na and Li ion diffusion in modified ASTM C 1260 test by Magnetic Resonance Imaging (MRI)

X. Feng [a,*], B.J. Balcom [b], M.D.A. Thomas [a], T.W. Bremner [a]

[a] Department of Civil Engineering, University of New Brunswick, Fredericton, NB, Canada
[b] MRI Center, Department of Physics, University of New Brunswick, Fredericton, NB, Canada

ARTICLE INFO

Article history:
Received 24 January 2008
Accepted 26 June 2008

Keywords:
Ion diffusion
Sodium
Lithium
MRI
Alkali-silica reaction

ABSTRACT

In the current study, MRI was applied to investigate lithium and sodium ion diffusion in cement paste and mortars containing inert sand and borosilicate glass. Paste and mortars were treated by complying with ASTM C 1260. Lithium and sodium distribution profiles were collected at different ages after different treatments. Results revealed that sodium ions had a greater diffusion rate than lithium ions, suggesting that Na reaches the aggregate particle surface before Li. Results also showed that Na and Li ions had a competitive diffusion process in mortars; soaking in a solution with higher [Li] favored Li diffusion but hindered Na diffusion. In mortars containing glass, a substantial amount of Li was consumed by the formation of ASR products. When [Li] in soaking solution was reduced to 0.37 N, a distinctive Na distribution profile was observed, indicating the free-state Na ions were continuously transformed to solid reaction products by ASR. Hence, in the modified ASTM C 1260 test, [Li] in the storage solution should be controlled at 0.74 N, in order to completely prevent the consumption of Na ions and thus stop ASR.

© 2008 Elsevier Ltd. All rights reserved.

1. Introduction

There are several standard laboratory testing methods to assess alkali-silica reaction, among which, ASTM C 1260 "Accelerated Detection of Potentially Deleterious Expansion of Mortar Bars Due to Alkali-Silica Reaction" is one of the most commonly used tests. It is based on the method developed by Oberholster and Davies [1] at the National Building Research Institute in South Africa.

In ASTM C 1260 and AASHTO T 303, the mortar bars are made with fine aggregate with a standard gradation. After 24 h, they are demolded, and then immediately placed in a storage container with sufficient tap water to totally immerse them. The container is then sealed and placed in an oven or water bath at 80 °C for a period of 24 h. After the bars are removed from the water, they are measured for initial length and then submersed in a 1 N NaOH solution at 80 °C, where they are stored for 14 days. Length change measurements are made periodically during this storage period. Typically the total expansion at the end of the 14-day soaking period is used in specifications, although the expansion limits specified by different agencies vary.

Although ASTM C 1260 was developed initially only to test aggregate reactivity, the test has been found to be a suitable method for assessing the effectiveness of supplementary cementing materials in reducing ASR expansion [2]. However, it is not suitable for evaluating the effects of lithium compounds in controlling ASR, for lithium would readily leach out of the bars when placed in water or 1 N NaOH solution. Thus the benefits of lithium would be lost without modifying the test. Therefore, in order to apply this test to lithium compounds, the soaking solutions should be modified by adding specified amounts of lithium to offset the leaching. However, there is little research regarding how the lithium and sodium distributions change during this test.

Magnetic Resonance Imaging (MRI) is a technique routinely used in medical imaging of the human body. In recent years, this technique has been employed at the MRI Centre of University of New Brunswick to explore chloride transport, sodium ion distribution, and water movement in cement and concrete materials [3,4]. In a recent study carried out at UNB, the possibility of using MRI to investigate lithium transport in mortars was evaluated by comparing the lithium ion concentration from Magnetic Resonance measurements and from Pore Solution Extraction [5,6]. The results suggested that the lithium (^{7}Li) determined by Magnetic Resonance represents only the free lithium contained in the pore solution and not that chemically bound by the cement hydrates.

In this study, the free lithium and sodium distribution profiles in cement paste, mortars containing inert sand, and mortars containing reactive silica were measured by MRI at different ages, after different treatments. These results will help understand the mechanism for the suppressive effects of lithium compounds on controlling ASR-induced expansion, and improve the testing method to assess the effectiveness of lithium compounds.

2. Materials and experimental details

A Type I Portland cement with a low Na_2Oe content of 0.43% was chosen for the current study. Its chemical composition is shown in

* Corresponding author. CTLGroup, Skokie, IL 60077, USA. Tel.: +1 847 972 3286.
E-mail address: XFeng@ctlgroup.com (X. Feng).

0008-8846/$ – see front matter © 2008 Elsevier Ltd. All rights reserved.
doi:10.1016/j.cemconres.2008.06.010

Table 1. The purpose for selecting such a low low-alkali cement was to minimize the influence of potassium on ASR while studying the Li and Na distributions in mortar samples by following the modified ASTM C 1260 test. USP-grade $LiNO_3$ and NaOH pellets were used as Li and Na sources, respectively. Graded Ottawa standard sand was chosen as the inert aggregate, crushed and graded borosilicate glasses having the same gradation as required in ASTM C 1260 as the reactive aggregate.

Cylindrical mortar specimens with a dimension of 43 mm diameter by ~30 mm long were made by complying with ASTM C 1260 requirements on sample preparation and curing conditions. The lithium contents in the mortar samples were controlled at 0 and 100% of standard lithium dose which gave a Li/[K+Na] molar ratio of 0.74 based on the cement equivalent soda content. The storage solutions were comprised of 1 N NaOH and 0.37 N, 0.74 N, or 1.0 N $LiNO_3$. In addition, two mortar specimens with inert sand but containing no Li in the mortars were also prepared, and were immersed in 1 N NaOH with 0.74 N $LiNO_3$, and 1 N NaOH with 1 N $LiNO_3$ solutions, respectively. The purpose of these specimens was to compare the diffusion rate of Li and Na ions at the same concentration level, and at 100% of the standard Li dose. Li MRI measurements were carried out at different stages of mortar treatments following ASTM C 1260 after demolding, 1 d in water, 3 d, 7 d, 14 d, 21 d and 28 d immersed in soaking solutions. Due to the low Na signal, no Na image was collected for treatments after demolding and 1 d in water. A paste specimen having a w/c ratio of 0.47 with 100% Li content was also prepared by rotating at approximately 2 rpm for the first 8 h to avoid segregation and was then treated in the same way as the mortar specimens. The detailed information about the specimens prepared for MRI measurements is given in Table 2.

In order to simplify the measurements and to easily interpret the ion distribution profiles, only one-dimensional images were collected. Therefore, after demolding, the circumferential surfaces of all testing specimens were sealed by a thick layer of ceramic epoxy to prevent the ingress of any ion when immersed in water and solutions, while the two end surfaces were exposed to the surrounding environment.

The distribution of Li was determined using the SPRITE MRI technique [7] with a field of view (FOV) of 100 mm acquired using 64 points, resulting in a nominal resolution of 1.5 mm. The SPRITE measurement parameters were set to t_p 30 μs, α 5°, and 5 T_1 50 ms. The total measurement time was approximately 35 min with 8192 signal averages. The measurements were acquired using a 2.4 T, 32-cm bore, superconducting magnet with a water-cooled gradient insert. A birdcage type probe was used for signal detection. The radio frequency amplifier was 2 kW. At this magnetic field, the resonance frequency of lithium was 38.54 MHz.

The centric scan, one-dimensional, DHK SPRITE (Double Half K Single-Point Ramped Imaging with T1 Enhancement) measurement was used to study the ingress of lithium. This measurement technique was selected due to the low absolute sensitivity of ^{7}Li (27% that of ^{1}H), the small amounts that are present and the short signal lifetimes (bulk T_1 of 10 ms and T_2* of 120 μs). In addition to the robust, quantitative nature of this technique, lithium is a quadrupolar nuclei and interpretation of the image intensity is more complex than spin 1/2 nuclei [8].

Table 1
Chemical composition of low-alkali cement

Oxide	%
SiO_2	20.53
Al_2O_3	5.97
Fe_2O_3	2.81
CaO	64.43
MgO	1.10
SO_3	3.21
Na_2O	0.20
K_2O	0.34
Na_2Oe	0.43
Loss on ignition	0.63

Table 2
Specimens prepared for MRI measurements

Specimen	Aggregate type	Li dose in specimen, %	Li dose in solution, %
Paste	–	100	100
Mortar 1	Inert	0	100
Mortar 2	Inert	0	135
Mortar 3	Inert	100	100
Mortar 4	Inert	100	50
Mortar 5	Glass	100	100
Mortar 6	Glass	100	50

The distribution of Na was also determined using the SPRITE MRI technique with a field of view (FOV) of 100 mm acquired using 64 points, resulting in a nominal resolution of 1.5 mm. The SPRITE measurement parameters were set to t_p 300 μs, α 49°. The total measurement time was approximately 45 min with 8192 signal averages. The same magnet as in the Li measurements with a different probe was used for the Na measurements. The resonance frequency of Na was 26.21 MHz.

It should be noted that the Li and Na ions measured by MRI are the free state of these ions, because the bound and solid forms have much shorter relaxation time which is not possible to be detected by MRI. In order to permit image scaling, Li and Na reference samples were put at the left side of test samples during image collection. The Li reference sample was a mixture of LiCl and $GdCl_3{\cdot}6H_2O$ solution. The Na reference sample was a mixture of NaCl and $MnSO_4$ solution.

3. Results and discussion

3.1. Na and Li ion diffusion in cement paste

Fig. 1 showed the one-dimensional SPRITE MRI profiles for Li and Na distributions obtained in the paste sample which contained 100% Li in the paste and immersed in 1 N NaOH and 0.74 N $LiNO_3$ solution. Based on the MRI theory, the signal intensity at any point in the images is proportional to the ion concentration [4,7]. The features at the left of the images are references that permit scaling. In Fig. 1a, the distribution of lithium in the paste is the region of the plot extending from approximately 50 mm to 80 mm. As the signal intensity is proportional to the lithium concentration in the sample, we interpret taking the relative loss or gain in the intensity after different treatments as the loss or gain in lithium concentration in the paste. For example, the total signal intensity after demolding was 4.6×10^6; after 1 d in water, it became 3.6×10^6, which is interpreted as 22% of lithium previously added in the paste had been either dissolved into the water surrounding phase or been bound by the cement hydration products. After 3 d immersion in 1 N NaOH and 0.74 N $LiNO_3$ solution, the intensity was 5.1×10^6, which means that the total lithium in the paste was 12% more than the original lithium content. The images clearly showed the lithium diffusion profiles at the two exposed end surfaces. The profiles for the two surfaces were fairly identical; suggesting that the slow rotation during sample preparation had successfully prevented any segregation. The paste sample was not fully saturated by lithium during the testing period up to 28 d.

It should be noted that in Fig. 1a, the lithium concentration at the two end surfaces increased with time. This is explained as the edge effect. At early times, the edge is saturated with Li but the saturated region is very thin. The resolution of the measurement is much coarser. We will therefore observe a low broad experimental profile at early exposure times, which will increase in height as lithium penetration occurs, and the region of high saturation increases.

Compared with the Li diffusion, Na penetrated much deeper into the paste than Li does (Fig. 1b). The specimen was almost fully saturated after 14 d immersion.

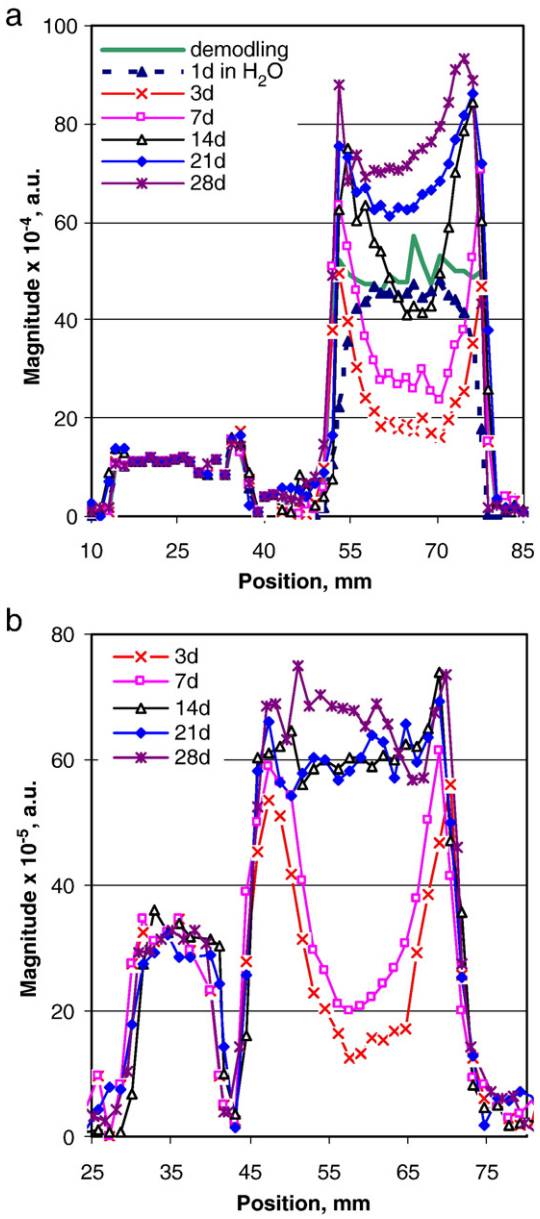

Fig. 1. a. One-dimensional SPRITE image of lithium distributions in cement paste with w/c=0.47 at demolding, 1 d in water, 3 d, 7 d, 14 d, 21 d, and 28 d immersed in 1 N NaOH and 0.74 N $LiNO_3$ solution. b. One-dimensional SPRITE image of sodium distributions in cement paste with w/c=0.47 at 3 d, 7 d, 14 d, 21 d, and 28 d immersed in 1 N NaOH and 0.74 N $LiNO_3$ solution.

3.2. Na and Li ion diffusion in mortars with inert sand

Fig. 2 shows the Li and Na distributions in mortar specimen with inert sand. No Li was added during the mortar preparation, and the soaking solution was comprised of 1 N NaOH and 0.74 N $LiNO_3$. As in the distribution profiles in Fig. 1, the features on left side of the images are the references of Li and Na, respectively. Compared with the ion distributions in cement paste (Fig. 1), both Li and Na ions penetrate significantly slower, corresponding to less diffusion paths in mortar than in cement paste. In addition, the Li distributions are not identical at the two end surfaces, with the one near the reference side having a much higher Li content than the other side. The first surface is the cast surface, which has a higher permeability due to the bleeding effect. Again, due to the edge effect explained in the above section, the surface concentration increased with time as well (Fig. 2a).

The Na signal intensity (Fig. 2b) contained much more noise compared to the signal intensity in the cement paste (Fig. 1b). It seemed that after 7 d, the casting surface had been fully saturated.

Fig. 3 shows the Li and Na distributions for the same mortar specimen as the previous one, but was immersed in 1 N NaOH and 1 N $LiNO_3$ solution. Again, the features on the left side of the images are the references of Li and Na, respectively. The figures showed that both the Li and Na distributions were comparable to the distributions for samples immersed in 1 N NaOH and 0.74 N $LiNO_3$ solution (Fig. 2). However, there were more Li ions penetrated into the specimen at the same depth, indicating soaking in more concentrated Li solution favored Li diffusion into the mortar. Furthermore, the Li distributions, again, are not identical at the two end surfaces, with the cast surface near the reference side having a much higher Li content than the other

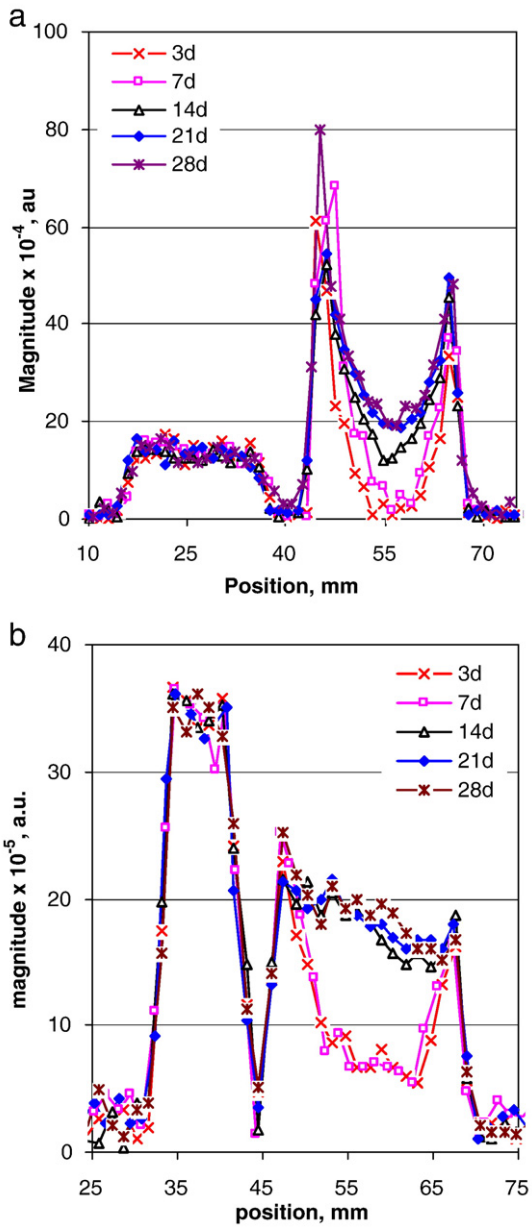

Fig. 2. a. One-dimensional SPRITE image of lithium distributions in mortar with inert sand and no Li at 3 d, 7 d, 14 d, 21 d, and 28 d immersed in 1 N NaOH and 0.74 N $LiNO_3$ solution. b. One-dimensional SPRITE image of sodium distributions in mortar with inert sand and no Li at 3 d, 7 d, 14 d, 21 d, and 28 d immersed in 1 N NaOH and 0.74 N $LiNO_3$ solution.

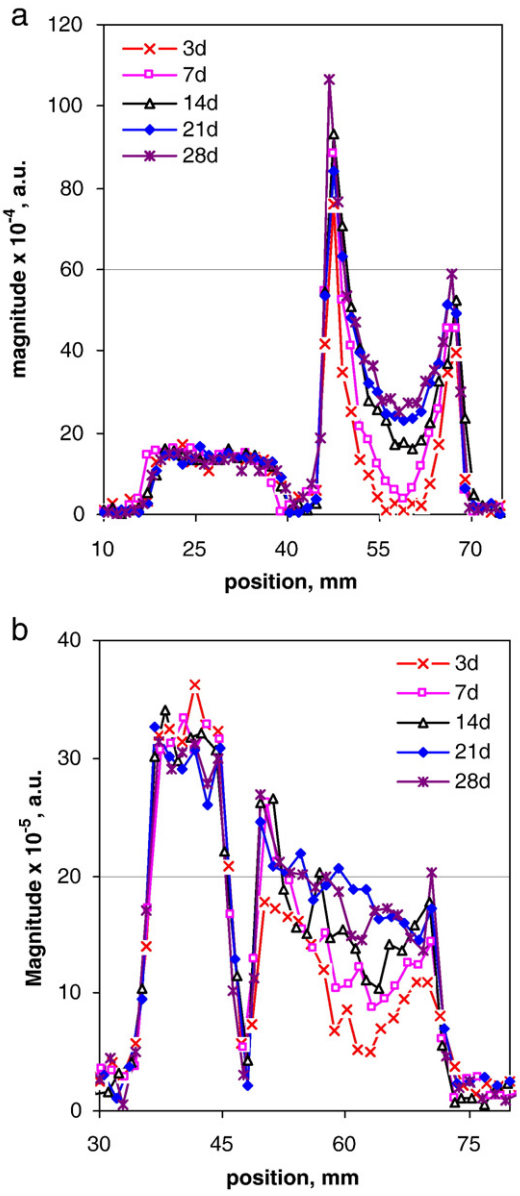

Fig. 3. a. One-dimensional SPRITE image of lithium distributions in mortar with inert sand and no Li at demolding, 1 d in water, 3 d, 7 d, 14 d, 21 d, and 28 d immersed in 1 N NaOH and 1 N $LiNO_3$ solution. b. One-dimensional SPRITE image of sodium distributions in mortar with inert sand and no Li at 3 d, 7 d, 14 d, 21 d, and 28 d immersed in 1 N NaOH and 1 N $LiNO_3$ solution.

surface. The increased surface concentration with time can also be explained by the edge effect.

The Na distributions in Fig. 3b showed the same trends as the mortar was immersed in 1 N NaOH and 0.74 N $LiNO_3$ (Fig. 2b). However, it took considerably more time to become fully saturated. After 14 d and 21 d, only the cast surface side reached fully saturation. These observations strongly suggested that Li and Na had a competition when diffusing into the mortars. A soaking solution with higher Li concentration favored the diffusion of Li ions, but hindered the diffusion of Na ions.

Fig. 4 shows the Li and Na distributions for the mortar specimen containing inert sand and a 100% Li dose that was immersed in 1 N NaOH and 0.74 N $LiNO_3$ solution. Again, the features on the left side of the images are the references of Li and Na, respectively. When the same method of calculation as that used for the paste sample was applied to this specimen, the total signal intensity after demolding was 2.1×10^6; after 1 d in water, it became 1.5×10^6. This suggests that 26% of the lithium previously added in the mortar had dissolved into water and/or been bound by cement hydration products. After 3 d immersion in 1 N NaOH and 0.74 N $LiNO_3$ solution, the intensity was 2.2×10^6, which means that the total lithium in the mortar was about 6.8% more than the original lithium content. The loss of Li when immersing in water for the mortar sample is on the same level as the loss for a paste sample, which had a 22% loss, but after 3 d immersion, much less Li penetrated into the mortar than into the paste, i.e., 6.8% vs 12%, due to less diffusion paths in the mortar sample. Again, the cast surface had a higher Li content than the other surface. The edge effect was more significant in this specimen than in the previous one.

As shown in Fig. 4b, mortar was fully saturated with Na ions after 14 d immersion. The differences between the cast surface and the bottom surface were noticeable.

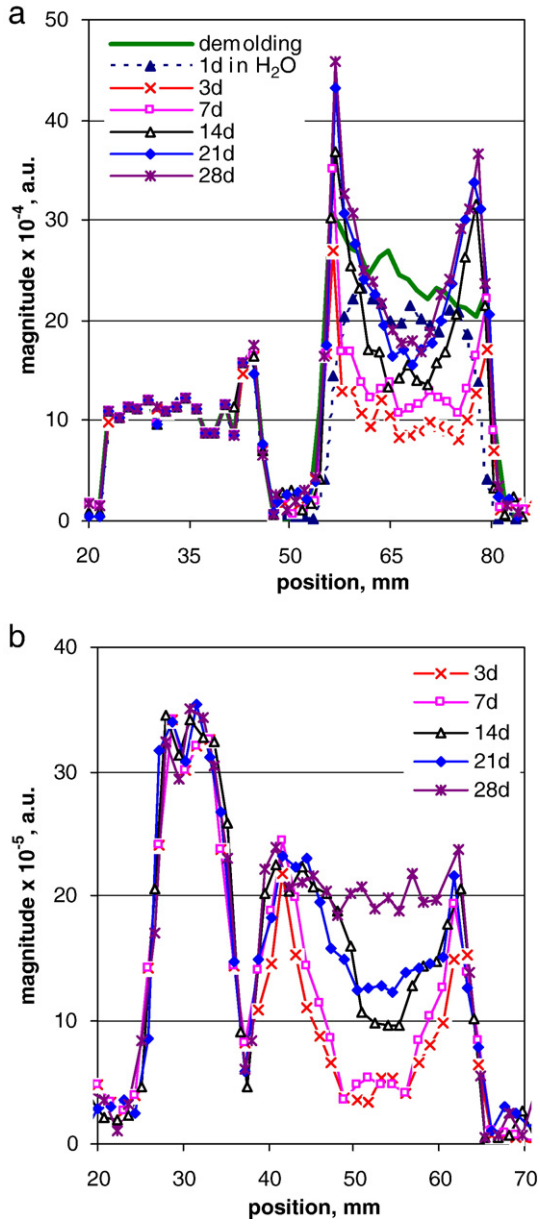

Fig. 4. a. One-dimensional SPRITE image of lithium distributions in mortar with inert sand and 100% Li at demolding, 1 d in water, 3 d, 7 d, 14 d, 21 d, and 28 d immersed in 1 N NaOH and 0.74 N $LiNO_3$ solution. b. One-dimensional SPRITE image of sodium distributions in mortar with inert sand and 100% Li at 3 d, 7 d, 14 d, 21 d, and 28 d immersed in 1 N NaOH and 0.74 N $LiNO_3$ solution.

Shown in Fig. 5a, when the Li concentration in the soaking solution was reduced to half (0.37 N), the Li distributions after demolding and 1 d in H_2O were identical to the previous sample, as they were from the same mixture. When immersed in solution, the penetration depths were less than soaking in 100% Li solution, and the Li contents at the same depth were considerably lower than the previous sample, although the Li contents at the two surfaces were very close. Regarding the loss and gain of Li, the total signal intensity after demolding was 2.2×10^6; after 1 d in water, it became 1.6×10^6, which could be interpreted as 28% of lithium previously added in the mortar had dissolved into the water and/or been bound by cement hydration products. After 3 d immersion in 1 N NaOH and 0.37 N $LiNO_3$ solution, the intensity was 2.3×10^6, which meant that the total lithium in the mortar was 3.9% more than the original lithium content. The loss of Li when immersing in water for the mortar sample is on the same level as the loss for the previous sample, which had a 26% loss, but after 3 d immersion, much less Li penetrated into the mortar than into the mortar soaked in solution with higher Li concentration, i.e., 3.9% vs 6.8%. This is reasonable, as the same amount of Li was added to both samples, therefore after 1 d in H_2O, the amounts of Li lost should be similar. But when immersed in the Li-containing solutions, higher Li concentration should favor the Li penetration into the mortars. This general rule was true as it was found that more Li penetrated into the mortar soaked in solution with higher Li concentration at the same penetration depth. However, it could not explain why both samples have the same Li intensity at the surface. These two mortar samples contained 100% Li, when they were exposed to Li-containing solutions, there probably were some interactions between the two parts of Li, which would affect the Li penetration chemically and physically, yielding a more complicated penetration profile. Therefore, unlike the mortar samples with no addition of Li (Figs. 2 and 3), the effects of the Li concentration in the soaking solutions on Li diffusion were ambiguous.

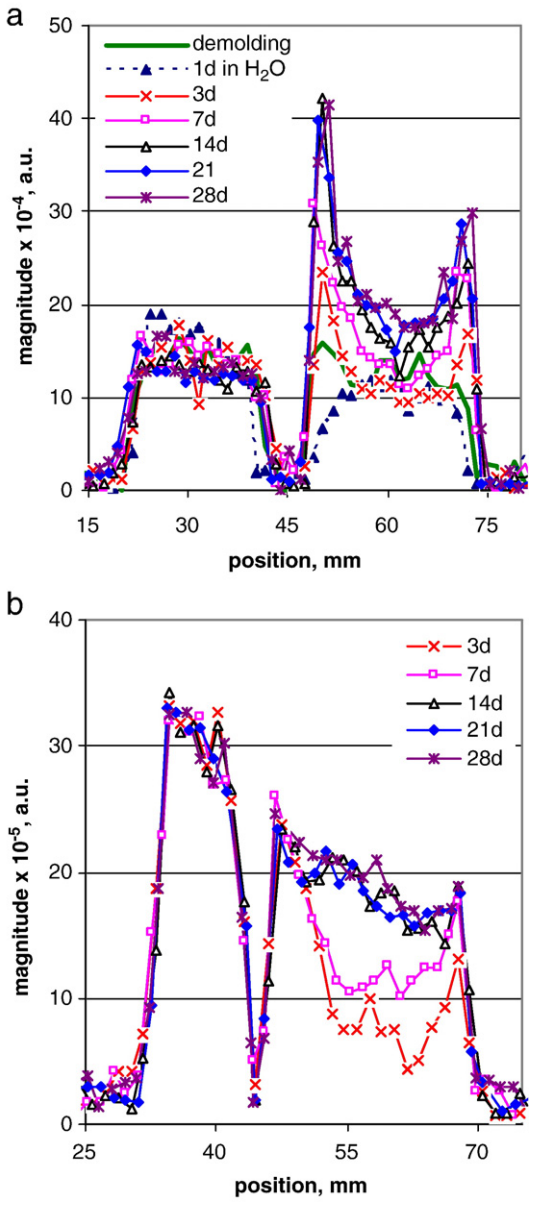

Fig. 5. a. One-dimensional SPRITE image of lithium distributions in mortar with inert sand and 100% Li at demolding, 1 d in water, 3 d, 7 d, 14 d, 21 d, and 28 d immersed in 1 N NaOH and 0.37 N $LiNO_3$ solution. b. One-dimensional SPRITE image of sodium distributions in mortar with inert sand and 100% Li at 3 d, 7 d, 14 d, 21 d, and 28 d immersed in 1 N NaOH and 0.37 N $LiNO_3$ solution.

The mortar was fully saturated with Na at 14 d immersion, as shown in Fig. 5b. The differences between the two end surfaces are more pronounced.

3.3. Na and Li ion diffusions in mortars with graded glass

Fig. 6 shows the Li and Na distribution profiles for the mortar where the inert sand was replaced by alkali alkali-silica reactive glass. From Fig. 6a, the total Li penetrated into the mortar was almost doubled compared to the mortar with inert sand. The signal intensity after demolding was 2.0×10^6; after 1 d in water, it became 1.5×10^6. This suggests that 25% of lithium previously added in the mortar had dissolved into the water and/or bound by cement hydration products. After 3 d immersion in 1 N NaOH and 0.74 N $LiNO_3$ solution, the intensity was 2.8×10^6, which meant that the total lithium in the mortar was about 36% more than the original lithium content. The loss of Li when immersing in water for the mortar sample is on the same level as the loss for mortars with inert sand, but after 3 d immersion, much more Li penetrated into the mortar than into the paste, i.e., 36% vs 6.8%. This was probably a result of Li consumption by the alkali alkali-silica reaction, which might change the mortar pore system.

The Na distribution, shown in Fig. 6b, had a similar trend as the mortar with inert sand, although one end surface was fully saturated only after 3 d immersion in solution, and it took 14 d to get fully saturated for the mortar with inert sand. These observations did not indicate a significant consumption of Na by the alkali alkali-silica reaction in the presence of lithium.

Fig. 7a shows that when the Li concentration in the soaking solution was reduced to half of the previous test, less Li penetrated into the mortar at 3 d and 7 d, but it reached the same level as the previous test at later ages. The signal intensity after demolding was 2.0×10^6; after 1 d in water, it became 1.4×10^6, which could be interpreted that about 30% of lithium previously added in the mortar had dissolved into the water and/or become bound by cement hydration products. After 3 d immersion in 1 N NaOH and 0.37 N $LiNO_3$ solution, the intensity was 2.8×10^6, which meant the total lithium in the mortar was about 25% more than the original lithium content. The loss of Li when immersing in water for the mortar sample is on the same level as the loss for previous mortar sample, as they were from the same mixture. But after 3 d immersion, much less Li penetrated into the mortar than into the previous one, i.e., 25% vs 36%. The diffusion profiles also showed that with soaking time, Li ions were not increased at the specimen central area, indicating that there was Li consumption at this location but the Li diffusion rate was too slow to compensate for the consumption. This consumption could result from the formation of Li-bearing reaction products. These observations also suggested that a solution with higher Li concentration favored the Li penetration, but had no influence on the Li surface concentration. This

was probably a consequence of the severe alkali alkali-silica reaction in the mortar, as the gel products and Li-containing products might block the pore system, thus Li ions could not penetrate as far as in the previous test.

A very distinctive behavior of the Na distribution in this specimen, different from all the previous tests, as shown in Fig. 7b, was that the Na hardly reached fully saturation even up to 28 d immersion. This drastic difference was introduced by the alkali alkali-silica reaction. With the progress of ASR, Na ions were continuously consumed within the mortar and were turned into solid gel products that were not detectable in MRI measurements, thus due to a Na concentration gradient between the solution and the mortar pore solution, Na ions would continuously penetrate into the mortar from the soaking solution, forming a diffusion profile. This finding further revealed that in the modified ASTM C 1260 test, the storage solution had to contain

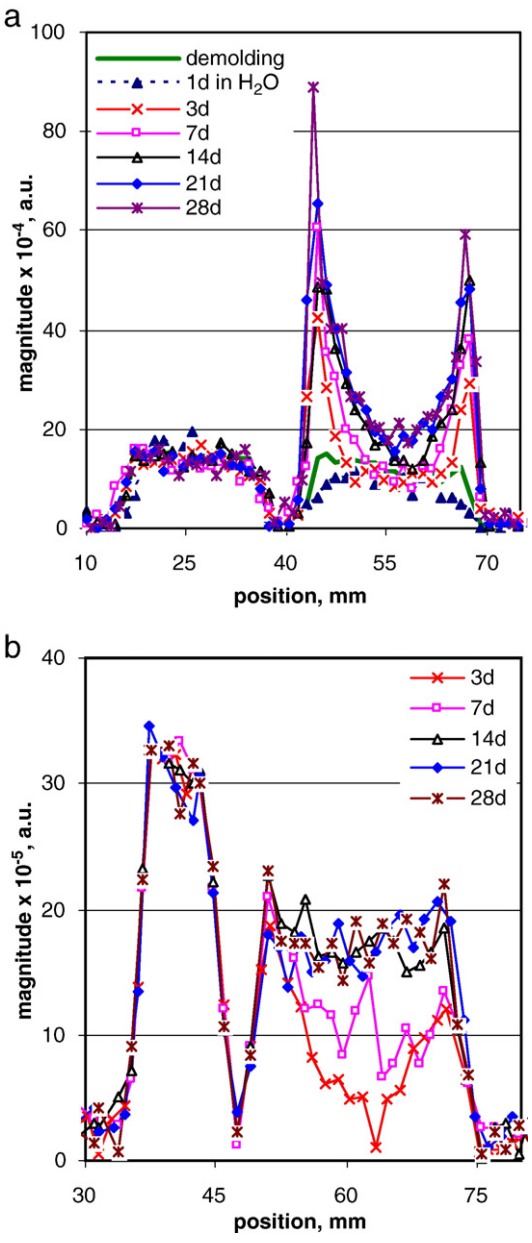

Fig. 6. a. One-dimensional SPRITE image of lithium distributions in mortar with glass and 100% Li at demolding, 1 d in water, 3 d, 7 d, 14 d, 21 d, and 28 d immersed in 1 N NaOH and 0.74 N $LiNO_3$ solution. b. One-dimensional SPRITE image of sodium distributions in mortar with glass and 100% Li at 3 d, 7 d, 14 d, 21 d, and 28 d immersed in 1 N NaOH and 0.74 N $LiNO_3$ solution.

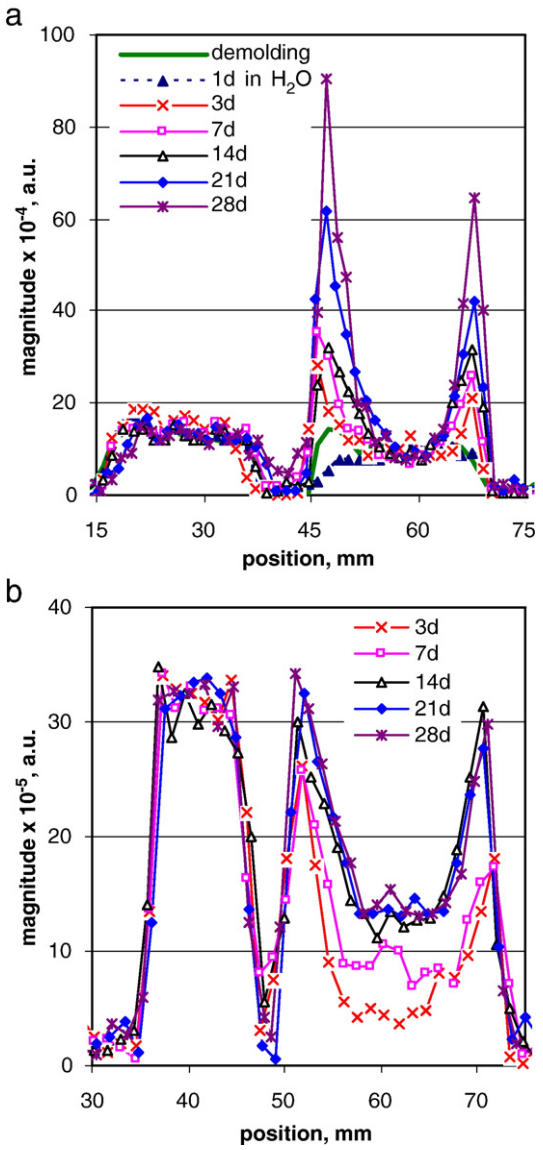

Fig. 7. a. One-dimensional SPRITE image of lithium distributions in mortar with glass and 100% Li at demolding, 1 d in water, 3 d, 7 d, 14 d, 21 d, and 28 d immersed in 1 N NaOH and 0.37 N $LiNO_3$ solution. b. One-dimensional SPRITE image of sodium distributions in mortar with glass and 100% Li at 3 d, 7 d, 14 d, 21 d, and 28 d immersed in 1 N NaOH and 0.37 N $LiNO_3$ solution.

100% Li dose to completely prevent the consumption of alkaline ions and thus stop the ASR.

4. Conclusions

1) Both Na and Li diffuse faster in paste than in mortar due to more diffusion paths in cement paste;
2) In all mortar samples, Na ions had a higher penetration rate than Li ions, suggesting that Na could reach the aggregate particles faster than Li;
3) In the modified ASTM C 1260 test, the Li and Na distributions of the mortar containing glass immersed in 100% Li solution were found to be similar to that of the mortars with inert sand. Whereas, a distinctive Na distribution profile was established when mortar was stored in half Li dose solution. This further confirmed that the storage solution must contain 100% Li in order to completely suppress ASR.

References

[1] E.R. Oberholster, G. Davies, An accelerated method for testing the potential reactivity of siliceous aggregates, Cement and Concrete Research 16 (1986) 181–189.
[2] M.D.A. Thomas, F.A. Innis, Use of the accelerated mortar bar test for evaluating the efficacy of mineral admixtures for controlling expansion due to alkali-silica reaction, Cement, concrete, and Aggregates 21 (1999) 157–164.
[3] D.S. Beyea, B.J. Balcom, T.W. Bremner, J.P. Prado, P.D. Green, L.R. Armstrong, E.P. Grattan-Bellow, Magnetic resonance imaging and content profiles of drying concrete, Cement and Concrete Research 28 (1998) 453–463.
[4] B.J. Balcom, C.J. Barrita, C. Choi, D.S. Beyea, T.W. Bremner, J.D. Goodyear, Single-point magnetic resonance imaging (MRI) of cement based materials, Materials and Structures 36 (2003) 166.
[5] J.J. Young, B.J. Balcom, T.W. Bremner, M.D.A. Thomas, K. Deka, A magnetic resonance imaging technique to determine lithium distribution in mortar, Proceedings of the 7th CANMET/ACI International Conference on Recent Advances in Concrete Technology, 2004, pp. 231–238.
[6] X. Feng, J.J. Young, M.D.A. Thomas, B.J. Balcom, T.W. Bremner, Lithium measurements by Magnetic Resonance Imaging and pore solution expression, The 12th International Conference on Alkali-Aggregate Reaction, 2004, pp. 501–511.
[7] B.J. Balcom, P.R. MacGregor, D.S. Beyea, P.D. Green, L.R. Armstrong, T.W. Bremner, Single Point Ramped Imaging with T1 Enhancement (SPRITE), Journal of Magnetic Resonance, Series A 123 (1996) 131–134.
[8] K. Deka, M.B. MacMillan, A.V. Ouriadov, I.V. Mastikhin, J.J. Young, P.M. Glover, G. Ziegler, B.J. Balcom, Quantitative density profiling with pure phase encoding and a dedicated 1D gradient, Journal of Magnetic Resonance 178 (2006) 25–32.